JOM, Vol. 68, No. 6, 2016
DOI: 10.1007/s11837-016-1940-z
© 2016 The Minerals, Metals & Materials Society

Effect of Microstructure on the Electro-Mechanical Behaviour of Cu Films on Polyimide

J. BERGER,[1] O. GLUSHKO,[1] V.M. MARX,[2] C. KIRCHLECHNER,[1,2] and M.J. CORDILL[1,3]

1.—Erich Schmid Institute of Materials Science, Austrian Academy of Sciences, and Department of Materials Physics, Montanuniversität Leoben, Jahnstrasse 12, 8700 Leoben, Austria. 2.—Max-Planck-Institut für Eisenforschung GmbH, Max-Planck-Str.1, 40237 Düsseldorf Germany. 3.—e-mail: megan.cordill@oeaw.ac.at

Metal films on polymer substrates are commonly used in flexible electronic devices and may be exposed to large deformations during application. For flexible electronics, the main requirement is to remain conductive while stretching and compressing. Therefore, the electro-mechanical behaviour of 200-nm-thick Cu films on polyimide with two different microstructures (as-deposited and annealed) were studied by executing in situ fragmentation experiments with x-ray diffraction, under an atomic force microscope, and with 4-point probe resistance measurements in order to correlate the plastic deformation with the electrical behaviour. The three in situ techniques clearly demonstrate different behaviours controlled by the microstructure. Interestingly, the as-deposited film with a bi-modal microstructure is more suited for flexible electronic applications than an annealed film with homogenous 1-μm-sized grains. The as-deposited film reaches a higher yield stress, with unchanged electrical conductivity, and does not show extensive surface deformation during straining.

INTRODUCTION

Today, a main field of application for thin films on polymer substrates is flexible electronics. Flexible electronics have been developed for various applications, including paper-like electronic displays, rollable solar cells and smart electronic textiles,[1–3] pursuing the aims of lightweight, low cost, and large area electronic devices. The systems may be exposed to repeated large deformations during manufacturing and usage. While the polymer substrates can easily recover from large deformations, thin metal or ceramic films often fail at low strains ($<2\%$). For optimal combined electro-mechanical properties, good adhesion and high fracture or yield strains (i.e. strains when the first cracks or localised deformation appear) are needed.[4,5] Thus, understanding the deformation behaviour of thin films on compliant substrates is crucial for improving the lifetime and future design of such electronic devices.

Ductile films, such as Ag, Au and Cu, deform plastically before through thickness cracks form, which is in contrast to brittle films (Cr, Ti, Ta) that crack at strains below 2%.[6–9] What is important for ductile films is how the microstructure affects the electro-mechanical behaviour and film deformation.[10–12] For ductile metal films bonded to a substrate, the geometric constraint caused by the substrate decelerates strain localisation. Hence, the metal film deforms uniformly to a large strain and this uniform deformation behaviour is important in order to achieve large failure strains. However, the failure strains of ductile films depend strongly on the film microstructure. A common methodology to measure the failure and adhesion of metal or ceramic films on polymer substrates is the fragmentation test, or a uniaxial tensile straining of a film–substrate system. The method has its origin in the determination of interfacial shear forces in fibre composite materials[13] and has been modified to apply to film–substrate systems.[5] Brittle films have been extensively studied with various in situ fragmentation experiments which utilised optical light microscopy,[14,15] scanning electron microscopy (SEM),[12,16] x-ray diffraction (XRD),[9,17,18] and 4-point probe (4PP) resistance measurements.[19,20]

(Published online May 9, 2016)

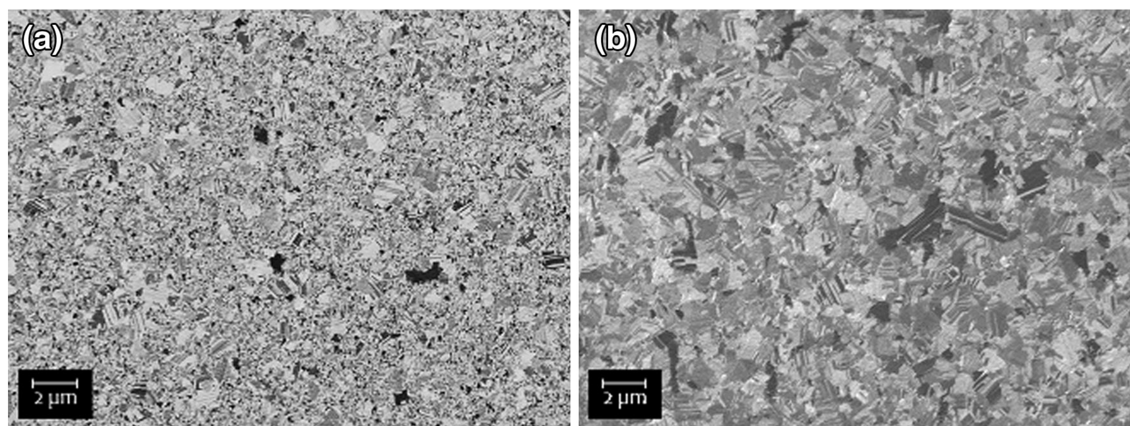

Fig. 1. Ion channelling contrast images of (a) as-deposited and (b) annealed 200-nm Cu film microstructures.

Ductile films, on the other hand, deform plastically via localised film thinning, commonly called necking, and is the first sign of yield that is best observed with in situ AFM in order to exploit the quantitative surface imaging technique that AFM provides.[21] With the AFM, first indications of localised plastic deformation (necks or necking) can be detected as a change in the surface height. In situ fragmentation testing with XRD and the $\sin^2\psi$ method[22] allows for microstructural influences to be studied. With the $\sin^2\psi$ method, the lattice strains are measured during straining and the stresses developing in the films can be calculated.[23] The technique has been utilised by several groups to study film thickness and microstructure effects on the mechanical behaviour.[12,24]

Despite the large number of different mechanical phenomena which may appear in a film during straining, the electrical resistance of the film is one of the most important parameters regarding the functional stability of the metallisations in flexible circuits and is directly influenced by the mechanical phenomena. Measuring the change of the resistance of a metal film can serve as a way to determine the presence of through-thickness cracks and, thus, failure properties. Strain-induced microstructural changes, such as the decrease of defect density or grain coarsening, might lead to a decrease of the electrical resistance, as reported in Ref. 25. Moreover, film thickness and grain size also have an impact on the electrical properties and have been studied.[11,20] However, these studies assumed that the electrical resistance is only affected by the formation of through-thickness cracks and do not consider the initial necking deformation. These studies also do not evaluate the resistance after unloading when the film is actually in a recovered state in which cracks and necks reconnect to allow current flow. In the study presented here, a comprehensive correlation between film microstructure, mechanical and electrical behaviour will be made by comparing two 200-nm Cu films. The as-deposited film has a bi-modal microstructure while the second film was annealed to achieve a homogenous 1-μm average grain size. In situ XRD, AFM and 4PP fragmentation experiments were carried out on both film systems to illustrate the fundamental and important role microstructure plays in flexible electronics, through the examination of mechanical damage and the resulting electrical behaviour.

EXPERIMENTAL

Two different thin film systems were produced for testing, an as-deposited 200-nm Cu film on polyimide, and an annealed 200-nm film that was heat treated at 200°C for 1 h after deposition without breaking vacuum. Both films were deposited using electron beam evaporation onto cleaned 50-μm UPILEX brand polyimide (PI) using a deposition rate of 5 Å/s. Samples sized 6 mm × 35 mm were cut out of the different Cu-PI sheets using a scalpel for fragmentation testing. The grain size of the films, both as-deposited and annealed, was characterised using SEM (Zeiss LEO 1525) and the TSL OIM Data Collection v.5.31 with electron backscatter diffraction (EBSD) scans and with ion channelling contrast images taken with the focused ion beam. Three EBSD scans were made on each film and the grain size and texture determined. The as-deposited films initially had a bi-modal grain size distribution with large 1-μm-sized grains embedded within a matrix of average 200-nm grains (Fig. 1a). A uniform microstructure was observed for the annealed Cu film with an average grain size of about 1 μm (Fig. 1b). No preferred orientation of the grains was found in either film.

In situ XRD fragmentation tests were performed at the synchrotron source BESSY II [Helmholtz-Zentrum Berlin für Materialien und Energie (HZB), Germany] on the beam line KMC-2[26] in order to measure the lattice strains and stresses of the Cu films during tensile straining. The tensile device was positioned so that the sample surface was in the reflection geometry to the incoming synchrotron x-ray beam. The sample was strained continuously

using a commercial Anton Paar TS 600® straining device to a maximum engineering strain of 12% and then unloaded to 0 N. The straining device recorded the load, displacement, and time of the whole sample (film and substrate) during the experiment. In situ measurements with a beam wavelength of 0.177 nm and a beam size of 300 μm in diameter were continuously performed at four different ψ angles with a Bruker VÅNTEC detector and an exposure time of 5 s. The lattice strains were calculated using the $\sin^2\psi$ method[22] and the peak shift utilising a Hill model with the x-ray elastic constants ($\frac{1}{2} S_2$)[23] for untextured (111) Cu reflections. From these experiments, stress–strain curves averaged over the beam footprint on the sample were calculated using Hooke's law, where the Cu film stresses obtained by the synchrotron data are plotted against the engineering strains measured with the tensile device.

For performing the in situ AFM fragmentation tests, a custom-built, miniaturised straining device was used and the experiments were performed in a similar manner as described in Refs. 18 and 21. All images were made with tapping mode and a scan size of 25 × 25 μm after increasing the strain in steps. Images were recorded of the same area for every straining step until the desired maximum strain was reached. Height images were analysed with Gwyddion,[27] using three vertical surface profiles (cross-sections) with approximately the same distance to each other across each image (approximately left, middle and right of the image). These profiles were positioned at nearly the same area for each straining step. With the aid of these profiles, the deformation spacing (distance between necks) was determined using the Δ/h approach described in Refs. 21 and 28.

Fragmentation tests with in situ resistance measurements were performed on an MTS Tyron 250® Universal testing machine using gauge length of 20 mm and a constant displacement rate of 5 μm/s for loading and unloading. For each film, four tests were executed, each to a maximum strain of 20%. The 4PP in situ resistance measurements were taken with a Keithley 2000 multimeter with the probing contacts incorporated into the grips.[19,29] A constant volume approximation was used to theoretically describe the electrical resistance change with increasing strain.[10,19] Not only was the resistance measured during the loading but also during unloading of the film to determine the amount of resistance recovery.[29] Finally, post-straining SEM of the resulting film surface deformation was performed.

RESULTS AND DISCUSSION

The in situ measurement of the Cu film stresses during straining reveal the expected trend. Before straining, the residual stresses were determined and the as-deposited film was stress free, while the annealed was compressive (approximately −250 MPa). Measuring the film stresses parallel to the straining direction (Fig. 2) shows the typical stress–strain curve for a ductile material. The stress in both films increases until a peak stress is reached, followed by a gradual decrease as the film uniformly deforms. The peak stresses could be considered the yield stresses of the films. As shown previously,[18] the shape of the stress–strain curve indicates that no through-thickness cracks have formed in the films. If through-thickness cracks were present, the stress would drop more dramatically due the fragmentation occurring the film. The peak stresses are reached at about 1% strain and they have different values due to the different microstructures. The as-deposited film with the bimodal microstructure has a peak stress at 900 MPa and the annealed film with a uniform microstructure reaches a lower peak stress at 750 MPa. Both film stresses decrease into the compressive regime during unloading and help with resistance recovery.[29]

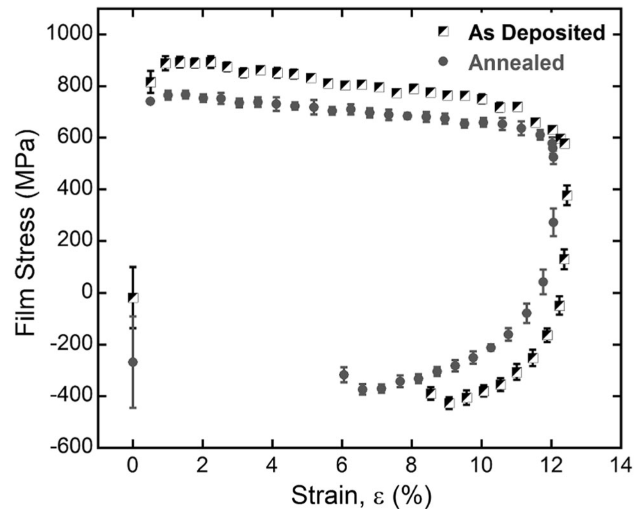

Fig. 2. Measured film stress–strain curves of the as-deposited and annealed films using XRD parallel to the straining direction. The points at zero strain are the measured residual stresses before straining.

In situ AFM fragmentation tests of as-deposited and annealed Cu films were performed to at least a strain of 15%. Comparing the height images taken at 15% strain (Fig. 3), it is evident that the annealed film exhibits more plastic deformation than the as-deposited film. Neither film showed through-thickness cracking up to this strain in agreement with the XRD results (Fig. 2). The deformation spacing is plotted as function of the strain for both films in Fig. 4. Necking initiates slightly earlier in the annealed film (1.4% strain) than in the as-deposited film (2% strain), and is most likely due to the larger initial grain size allowing for easier dislocation movement. A saturation regime is reached earlier for the annealed film (approximately 5% strain)

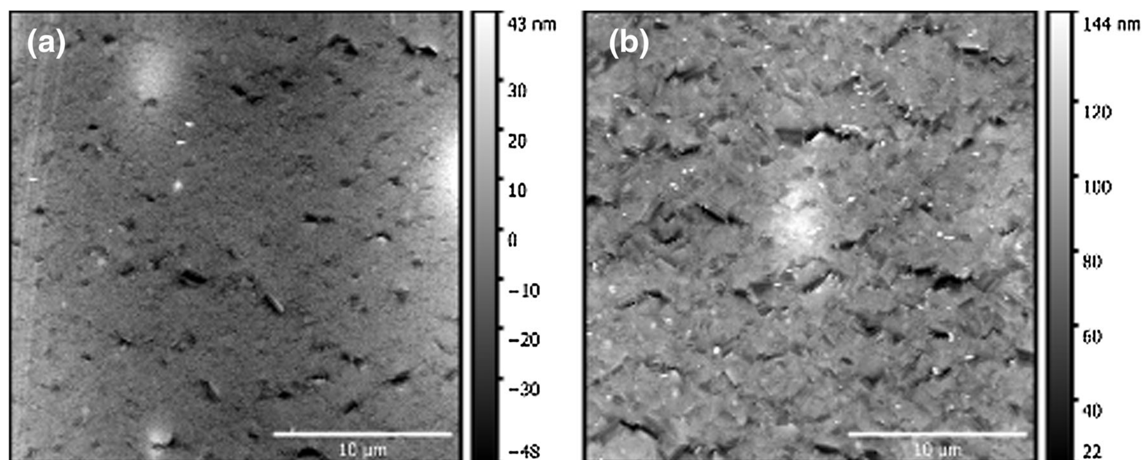

Fig. 3. AFM height images with surface profiles of the (a) as-deposited and (b) annealed 200-nm-thick Cu films at 15% strain. Note the different height scales used in the AFM images. The straining direction is in the vertical direction.

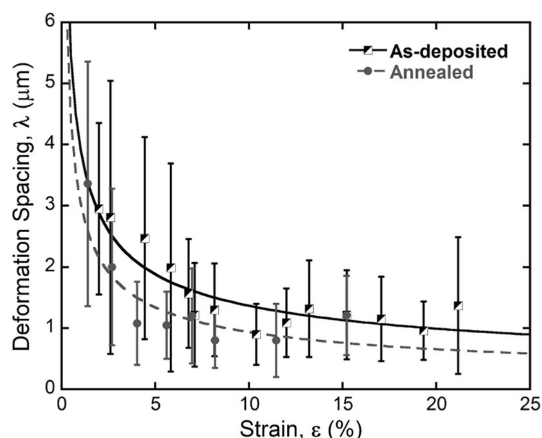

Fig. 4. Deformation spacing as a function of strain for the as-deposited and an annealed Cu films. The trend lines are only used to guide the eye and have no mathematical relationship.

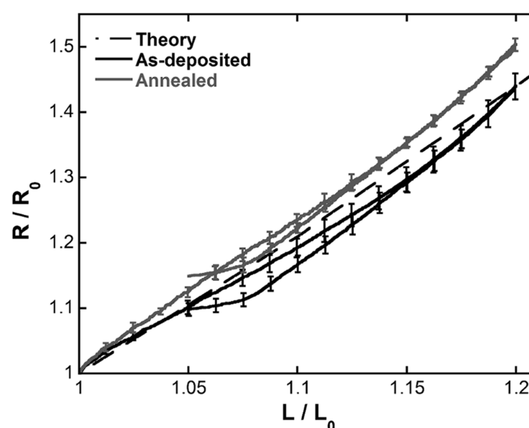

Fig. 5. Change of the relative resistance, R/R_0, with increasing relative length, L/L_0, of as-deposited and annealed Cu films. Error bars are the standard deviation of four experiments. The dotted line describes the constant volume assumption.

while the as-deposited film does not achieve a deformation spacing saturation until about 10% strain. The average deformation spacing at saturation is approximately the same for both films (1.1 ± 0.2 μm) and is due to fact that the film thickness is the same for both films. The microstructure only effects the initial yielding and not the deformation spacing which is known to be thickness-dependent.

The in situ 4PP experiments tie together the mechanical deformation observed with the in situ XRD and AFM experiments. As illustrated in Fig. 5, with increasing strain the relative resistance of both films rises constantly following the theoretical trend line (dashed line). The slope of the annealed curve is just slightly higher than the as-deposited curve. Due to the fact that neither curve deviates from the constant volume assumption, through-thickness cracking of the films was not expected nor observed with the AFM experiments. At the maximum strain, the average electrical resistance, $R_{\max}$, is 44% higher for the as-deposited samples and 51% higher for the annealed specimens than the average initial resistance.

During unloading, a decrease of resistance is observed. It is evident from Fig. 5 that at the beginning of unloading the relative resistance follows exactly its loading line for both samples. The annealed film does not show a full recovery of the resistance as compared to the as-deposited films which has improved resistance after straining. For the as-deposited film, the average final resistance of the samples, R_{f}, is about 10% higher than the initial resistance, R_0, and, for the annealed film, it is even 15% higher. The unloading can be correlated to the XRD experiments where the films go into compression causing any deformation, necks in the case here, to compress together and return the resistance

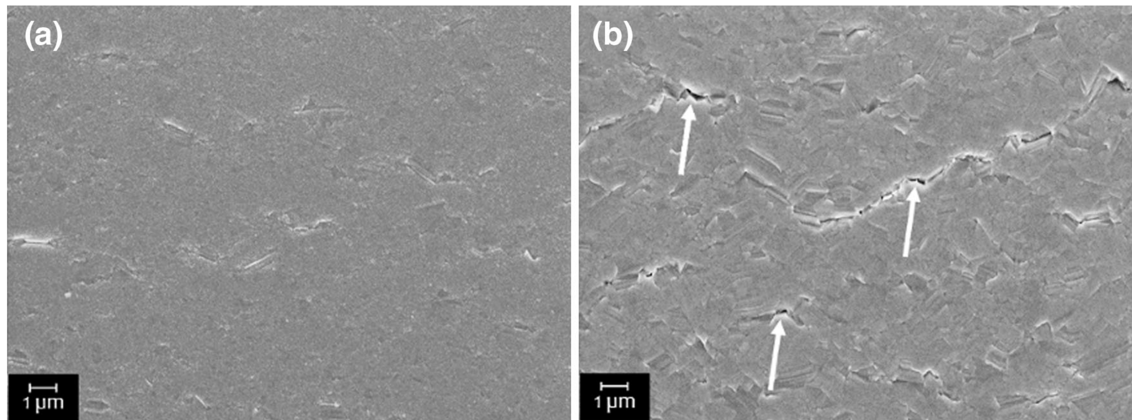

Fig. 6. Post-straining SEM images of the films strained to 20% with the 4PP. (a) As-deposited film and (b) annealed film with arrows indicating possible through thickness cracks. The straining direction is in the vertical direction.

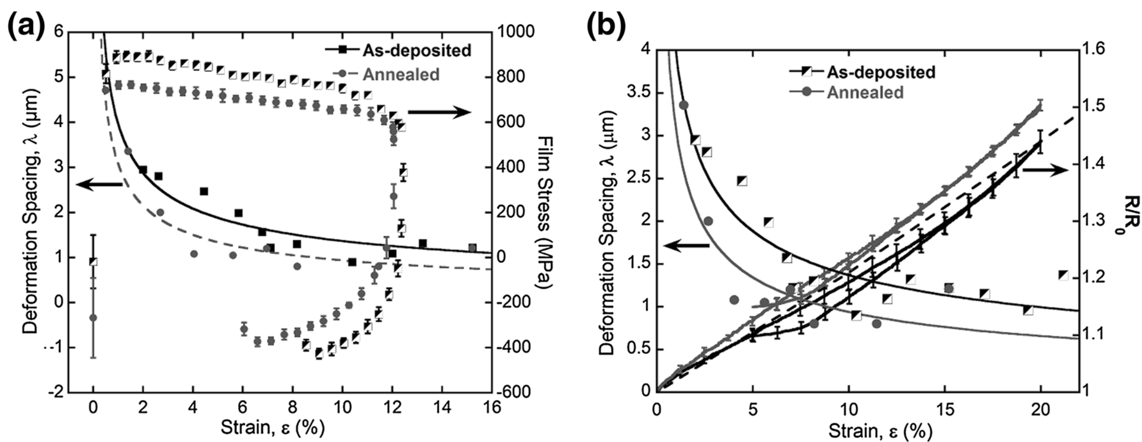

Fig. 7. Comparison of the electrical and mechanical deformation behaviour as a function of strain for 200-nm-thick Cu films on PI with different microstructures. (a) The stresses and deformation spacing results correleate at yielding and that no through-thickness cracks formed. (b) Comparison of the deformation spacing and resistance ratio also indicate that film deformation and cracking are connected.

close to its original state. Necking deformation produced during straining affects the uniform microstructure of the annealed film more than the as-deposited bi-modal structure. As shown previously,[25] the resistance recovery of the as-deposited film could be due to possible grain growth or the removal of vacancies within the film; however, these could not be confirmed with the experiments presented here and are only possible theories. The annealed film has a uniform microstructure but is always slightly above theory. This could be due to the large surface roughening that formed during straining (Fig. 2b). Both films would be considered acceptable under the electrical failure criterion (25% increase of R/R_0,[30]) and could be strained above 10% before electrical failure occurs similar to what was found in Ref. 11. However, as shown here, the as-deposited film reaches a slightly higher strain than the annealed. These electrical results are good for stretch-to-connect applications where straining is necessary for connecting parts.

Post-straining SEM imaging of the films strained to 20% (Fig. 6) with 4PP illustrate similar surface features as the AFM results. Both films have areas of necking with more surface roughening found for the annealed film (Fig. 6b). In the as-deposited film the necking is most likely located in the larger grains, as previously found.[18] Of note is the appearance of through-thickness cracks (arrows) in the annealed film with the additional 5% strain these samples endured compared to the in situ AFM experiments that were only strained to 15%.

It has been demonstrated that the 200-nm films behave in a completely ductile manner. Combining the results from the three in situ experiments (Fig. 7), several correlations can be drawn. First, comparing the film stress and deformation spacing data (Fig. 7a), the peak stresses were reached just prior to the strain at which deformation was observed with AFM (1% strain). If the peak stresses were to be considered the yield stresses of the films, then the Hall–Petch theory can be applied. Recall that the

annealed film with the uniform 1-μm average grain size had a lower peak stress (750 MPa) and deformation was observed at a lower strain (1.4% strain) compared to the as-deposited film (900 MPa and 2% strain) with the large grains embedded in the 200 nm grain matrix. With continued straining, the stresses do not dramatically decrease, indicating that through-thickness cracks have not formed, as illustrated by the observation of only necks with the in situ AFM experiment. The comparision of the electrical data and mechanical data (Fig. 7b) also provide the same conclusion that through-thickness cracks have not formed, since the R/R_0 values follow the theoretical line well up to 20% strain. At low strains, necking occurs as known by the in situ AFM experiments and does not greatly influence the electrical resistance. Even when the deformation spacing reaches the saturation regime between 5% and 10% strain, the electrical resistance is not greatly affected. After 20% strain, through-thickness cracks might be present in the annealed film (Fig. 6b) and the increased deviation from theory may be an indication. Evidence of through-thickness cracks were not confirmed with the in situ AFM experiment because the whole sample broke after 15% strain. It should be noted that when only in situ electrical measurements are utilised, information can be lost on how the film deforms and how that deformation directly relates to electrical behavior. Fragmentation tests of ductile films would be best performed utilising two in situ methods (i.e. 4PP and AFM, or 4PP and XRD) in order to determine exactly how the deformation is influencing the electrical behaviour.[31] This was shown to be a good method for 200-nm sputter-deposited Cu films on polyethylene terephthalate, which determined that through-thickness cracks did not form until the saturation deformation spacing was achieved, and only then did the electrical resistance deviate from theory.

CONCLUSION

A smaller grain size has been shown to better withstand electro-mechanical failure than a coarser-grained microstructure for conductive metallisations in flexible electronics. Coarse-grained (annealed) films promote earlier deformation during mechanical straining and have a lower yield stress, more surface roughening and less resistance recovery compared to the as-deposited microstructure. The as-deposited microstructure increases the yield stress described by the Hall–Petch theory and reduces the amount of deformation with fewer micron-sized grains with easy dislocation glide. In terms of the electrical behaviour, the as-deposited structure can recover more resistance due to possible strain-induced grain growth. The combination of higher yield stress, more electrical recovery and less deformation illustrate that microstructure is very important and smaller grain sizes are ideal for improved reliability of flexible electronics.

ACKNOWLEDGEMENTS

Funding of the research has been provided by the Austrian Science Foundation (FWF) through Project P22648-N20. The authors would like to thank the HZB for the allocation of synchrotron radiation beamtime and thankfully acknowledges the financial support by the HZB (Project No. 2011_2_110211 and 2012_1_111115). The authors would like to also thank I. Zizak and D. Többens, of the HZB for beamline support and J. Schalko of the Research Unit for Integrated Sensor Systems of the Austrian Academy of Sciences (Wiener Neustadt, Austria) for providing the Cu films.

REFERENCES

1. A.C. Siegel, S.T. Phillips, M.D. Dickey, N. Lu, Z. Suo, and G.M. Whitesides, *Adv. Funct. Mater.* 20, 28 (2010).
2. G. Kettlgruber, M. Kaltenbrunner, C.M. Siket, R. Moser, I.M. Graz, R. Schwödiauer, and S. Bauer, *J. Mater. Chem. A* 1, 5505 (2013).
3. Q. Cao, S.-H. Hur, Z.-T. Zhu, Y.G. Sun, C.-J. Wang, M.A. Meitl, M. Shim, and J.A. Rogers, *Adv. Mater.* 18, 304 (2006).
4. M.J. Cordill, *JOM* 62, 9 (2010).
5. D.C. Agrawal and R. Raj, *Acta Metall.* 37, 1265 (1989).
6. M.J. Cordill, A. Taylor, J. Schalko, and G. Dehm, *Metall. Mater. Trans. A* 41, 870 (2010).
7. M.J. Cordill, A.A. Taylor, J. Berger, K. Schmidegg, and G. Dehm, *Philos. Mag.* 92, 3346 (2012).
8. A.A. Taylor, M.J. Cordill, L. Bowles, J. Schalko, and G. Dehm, *Thin Solid Films* 531, 354 (2013).
9. S. Frank, U.A. Handge, S. Olliges, and R. Spolenak, *Acta Mater.* 57, 1442 (2009).
10. N. Lu, X. Wang, Z. Suo, and J.J. Vlassak, *Appl. Phys. Lett.* 91, 221909 (2007).
11. N. Lu, X. Wang, Z. Suo, and J. Vlassak, *J. Mater. Res.* 24, 379 (2009).
12. J. Lohmiller, N.C. Woo, and R. Spolenak, *Mater. Sci. Eng. A* 527, 7731 (2010).
13. A. Kelly and W.R. Tyson, *J. Mech. Phys. Solids* 13, 329 (1965).
14. J. Andersons, Y. Leterrier, G. Tornare, P. Dumont, and J.A. Månson, *Mech. Mater.* 39, 834 (2007).
15. W.P. Vellinga, J.T.M. De Hosson, and P.C.P. Bouten, *J. Appl. Phys.* 112, 083520 (2012).
16. N.C. Woo, K. Cherenack, G. Tröster, and R. Spolenak, *Appl. Phys. A* 100, 281 (2010).
17. P.A. Gruber, C. Solenthaler, E. Arzt, and R. Spolenak, *Acta Mater.* 56, 1876 (2008).
18. V.M. Marx, F. Toth, A. Wiesinger, J. Berger, C. Kirchlechner, M.J. Cordill, F.D. Fischer, F.G. Rammerstorfer, and G. Dehm, *Acta Mater.* 89, 278 (2015).
19. O. Glushko and M.J. Cordill, *Exp. Tech.* (2014). doi:10.1111/EXT.12082.
20. N. Lu, Z. Suo, and J.J. Vlassak, *Acta Mater.* 58, 1679 (2010).
21. M.J. Cordill and V.M. Marx, *Philos. Mag. Lett.* 93, 618 (2013).
22. L. Spieß, G. Teichert, R. Schwarzer, H. Behnken, and C. Genzel, *Moderne Röntgenbeugung* (Wiesbad: Teubner, 2005).
23. I.C. Noyan and J.B. Cohen, *Residual Stress: Measurement by Diffraction and Interpretation* (New York: Springer, 2013).
24. P.A. Gruber, E. Arzt, and R. Spolenak, *J. Mater. Res.* 24, 1906 (2009).
25. O. Glushko and M.J. Cordill, *JOM* 66, 1 (2014).
26. A. Erko, I. Packe, C. Hellwig, M. Fieber-Erdmann, O. Pawlizki, M. Veldkamp, and W. Gudat, *AIP Conf. Proc. 521* (Melville, NY: AIP Publishing, 2000), pp. 415–418.

27. D. Nečas and P. Klapetek, *Open Phys.* 10, 181 (2012).
28. M.J. Cordill and V.M. Marx, *MRS Proc.* 1527, 2 (2013).
29. O. Glushko, V.M. Marx, C. Kirchlechner, I. Zizak, and M.J. Cordill, *Thin Solid Films* 552, 141 (2014).
30. G.-D. Sim, Y.-S. Lee, S.-B. Lee, and J.J. Vlassak, *Mater. Sci. Eng. A* 575, 86 (2013).
31. M.J. Cordill, O. Glushko, J. Kreith, V.M. Marx, and C. Kirchlechner, *Microelectron. Eng.* 137, 96 (2014).